

DUAL ENERGY MAMMOGRAPHY: EVALUATION OF SCINTILLATORS FOR X-RAY DETECTORS USING A SIGNAL TO NOISE RATIO MODEL

Adrianos Toutountzis^{a,b}, Nikolaos Stathonikos^a, Giorgos Fountos^a,
Giorgos Nikiforidis^b, Ioannis Kandarakis^a

^a Department Medical Instruments Technology, Technological Educational Institution
of Athens, Ag. Spyridonos, Aigaleo, 122 10 Athens, Greece

^b Department of of Medical Physics, Medical School, University of Patras, 265 00
Patras, Greece

- Corresponding author: kandarakis@teiath.gr

Keywords: dual energy, mammography, noise, SNR, GdOS, LSO.

Abstract. *The purpose of this study was to perform an analysis on microcalcification visualization in dual energy subtraction mammography. A theoretical model was applied in order to evaluate the signal to noise ratio on subtracted mammographic images. The detector performance is investigated and compared for two different scintillators; the commercially used GdOS:Tb, and LSO:Ce. In addition, the estimation of signal and noise levels is performed for different tissue compositions and various x ray spectra. The image parameters were selected for the optimization of a dual energy subtraction technique for the improved detection and visualization of microcalcifications. The results are presented and the dependence on image parameters is discussed.*

1. Introduction

During the past decade digital X ray imaging has lead to a variety of new medical imaging applications such as dual energy x-ray mammography. The latter seems to be an innovative technique in specific tissue imaging, like microcalcification or soft tissue visualization. In addition, conventional mammography does not provide adequate information for tissue characterization such as differentiation between benign and malignant tumors. With dual energy technique, high and low energy images are separately acquired and “subtracted” from each other in a weighted manner to cancel out the cluttered tissue structure so as to decrease the obscurity from overlapping tissue structures.

The information derived from a dual energy mammography can be evaluated by estimating the noise levels in the final subtracted image. Thus signal to noise (SNR) analysis is necessary to provide data for imaging performance and the optimization of the dual exposure parameters used.

Previous studies on this subject have been reported^[1,2] for systems based mainly on the commercially available Thallium activated Cesium Iodide (CsI:Tl) and Terbium activated Gadolinium Oxysulfide (Gd₂O₂S:Tb) scintillators. In the present paper a dual energy signal to noise analysis was performed for Cerium activated Lutetium Oxyorthosilicate (Lu₂SO₅:Ce) scintillator which is widely used in PET

detectors, and has been recently studied for x-ray mammography applications^[3,4], exhibiting suitable imaging performance.

2. Materials and Methods

Assuming a compressed breast of total thickness T , composed by three types of tissue: adipose, glandular and microcalcification, with thicknesses t_a , t_b and t_c respectively. The mean measured signals for the high and low energy will therefore be^[1]:

$$S_j = \int dE \cdot d^2 \cdot \Phi_j(E) \cdot e^{-\mu_a(E)t_a - \mu_b(E)t_b - \mu_c(E)t_c} \cdot A(E) \cdot Q(E) \quad (1)$$

where j denotes the high or low energy, $\Phi_j(E)$ is the low or high energy spectrum in terms of photon fluence (photons/mm²), $\mu(E)$ is the energy dependent linear attenuation coefficient for the three types of tissue a, b, c, $A(E)$ is the detector quantum efficiency of the scintillator as a function of photon energy and $Q(E)$ is the detector gain and represents the signal generated by each detected X ray photon.

The detector quantum efficiency, which is the fraction of incident photons interacting with the scintillator, was calculated using the following equation:

$$A(E) = 1 - e^{-\mu_s(E)t_s} \quad (2)$$

$\mu(E)_s$ is the linear attenuation coefficient of the scintillator used for the conversion of X rays to optical photons.

The energy dependent detector gain is a factor which describes the signal generated per absorbed x ray photon, taking into account performance characteristics of the scintillator coupled with an optical detector and is expressed as:

$$Q(E) = n_c \frac{E}{E_{Optical}} g_{\Lambda} a_s \quad (3)$$

n_c is the intrinsic conversion efficiency, expressing the fraction of absorbed x rays converted into light within the scintillator material, $E_{Optical}$ is the peak value of the emitted light spectrum expressed in eV, g_{Λ} is the light attenuation coefficient and a_s is the spectral matching factor, expressing the spectral compatibility of the emitted light spectrum with the spectral sensitivity of the optical detector.

Defining $\Delta\mu_b(E) = \mu_b(E) - \mu_a(E)$ and $\Delta\mu_c(E) = \mu_c(E) - \mu_a(E)$, the unsubtracted image signal to noise ratio, for high or low energy X rays, is defined by the equation:

$$SNR_{S_j} = \frac{\int dE \cdot d^2 \cdot \Phi_j(E) \cdot e^{-\mu_{av}(E)T} \cdot e^{-\Delta\mu_b(E)t_b - \Delta\mu_c(E)t_c} \cdot A(E) \cdot Q(E)}{\sqrt{\int dE \cdot d^2 \cdot \Phi_j(E) \cdot e^{-\mu_{av}(E)T} \cdot e^{-\Delta\mu_b(E)t_b - \Delta\mu_c(E)t_c} \cdot A(E) \cdot Q^2(E)}} \quad (4)$$

According to the formalism made by Lemacks *et al*^[1], the overall dual energy subtracted image SNR for glandular tissue or microcalcification cancellation is:

$$SNR_{t_i} = \frac{t_i}{\sqrt{\frac{k_{il}^2}{SNR_{Sl}^2} + \frac{k_{ih}^2}{SNR_{Sh}^2}}}, \quad i = b, c \quad (5)$$

In equation (4) the numerator represents the signal for the granular or the microcalcification (*b* or *c* respectively) and the denominator denotes the square root of the noise variance; the coefficients k_{ij} are combinations of differences between the adipose, glandular tissue and microcalcification linear attenuation coefficients, averaged over the detected energy spectrum:

$$k_{bl} = \frac{\overline{\Delta\mu_{ch}}}{\overline{\Delta\mu_{bl} \Delta\mu_{ch} - \Delta\mu_{cl} \Delta\mu_{bh}}}, \quad k_{bh} = \frac{-\overline{\Delta\mu_{cl}}}{\overline{\Delta\mu_{bl} \Delta\mu_{ch} - \Delta\mu_{cl} \Delta\mu_{bh}}} \quad (6)$$

$$k_{cl} = \frac{-\overline{\Delta\mu_{bh}}}{\overline{\Delta\mu_{bl} \Delta\mu_{ch} - \Delta\mu_{cl} \Delta\mu_{bh}}}, \quad k_{ch} = \frac{\overline{\Delta\mu_{bl}}}{\overline{\Delta\mu_{bl} \Delta\mu_{ch} - \Delta\mu_{cl} \Delta\mu_{bh}}}$$

For the calculation of signal to noise ratio, a compressed breast thickness of 5 cm was assumed, consisting of 50% adipose and 50% glandular tissue and microcalcification size ranging from 100 μm to 500 μm .

The incident x ray photon fluence used for equations (1) and (4), was calculated using a theoretical model^[5] that describes the energy spectral distribution of x rays produced by a molybdenum, rhodium and tungsten anode target. The x ray attenuation for the formation of the mean measured signal, as well as for the quantum detection efficiency and the final signal to noise ratio, were calculated by considering exponential X ray absorption within the tissue and the scintillator material. The linear attenuation coefficients for the adipose and glandular tissue (ICRU-44), for the microcalcifications hydroxyapatite [$Ca_5(PO_4)_3(OH)$] and for LSO:Ce and GdOS:Tb scintillating materials were obtained from data tabulated by NISTR^[6].

The following table shows the values of various parameters for GdOS:Tb and LSO:Ce, such as density, intrinsic conversion efficiency^[4,7], peak value of the light emission spectrum in nanometers and spectral compatibility with amorphous silicon flat panel detector.

	GOS	LSO
ρ	7.44	7.4
η_c	0.2	0.102
λ	545	420
a	0.92	0.58

Table 1 : Scintillator parameters

Using relations (1), (2) and (3), the mean measured signals for the high and the low energy may be calculated as a function of x ray photon energy and depend on the detector intrinsic parameters. The final expression for the subtracted calcification signal to noise ratio depends directly on the microcalcification thickness, the low and high energy SNR and various combinations of attenuation coefficient differences averaged over the spectra.

3. Results and Discussions

Calculations were performed for various combinations of tissue composition and high x ray tube voltages, anode targets, filters and for both GdOS and LSO scintillators. In the following tables we can see the SNR for microcalcification signal in subtracted images for high and low energy images using GdOS and LSO scintillator.

Combination of HE – LE Anode/Filter/Voltage	Exposure of HE - LE	Microcalcification size in μm								
		100	150	200	250	300	350	400	450	500
Mo/Mo/40 – Mo/Mo/20	1.441 – 0.15	0.05	0.07	0.09	0.11	0.13	0.15	0.17	0.19	0.21
Mo/Mo/40 – Mo/Mo/25	1.441 – 0.36	0.05	0.08	0.11	0.13	0.16	0.18	0.21	0.23	0.26
Mo/Mo/40 – Mo/Mo/30	1.441 – 0.641	0.04	0.05	0.07	0.09	0.11	0.13	0.14	0.16	0.18
Mo/Mo/40 – Rh/Rh/20	1.441 – 0.095	0.45	0.67	0.89	1.1	1.31	1.52	1.72	1.92	2.12
Mo/Mo/40 – Rh/Rh/25	1.441 – 0.231	0.98	1.46	1.94	2.41	2.88	3.34	3.79	4.24	4.69
Mo/Mo/40 – Rh/Rh/30	1.441 – 0.424	1.56	2.33	3.09	3.85	4.6	5.34	6.07	6.8	7.52
Mo/Mo/40 – Rh/Rh/35	1.441 – 0.666	2.1	3.13	4.16	5.17	6.18	7.18	8.17	9.15	10.12
Mo/Mo/40 – Rh/Rh/40	1.441 – 0.948	2.55	3.81	5.06	6.29	7.52	8.73	9.94	11.14	12.32
Mo/Mo/40 – W/La/20	1.441 – 0.687	0.14	0.2	0.27	0.34	0.4	0.46	0.52	0.58	0.64
Mo/Mo/40 – W/La/25	1.441 – 1.466	0.11	0.17	0.23	0.28	0.33	0.39	0.44	0.49	0.54
Mo/Rh/40 – Rh/Rh/20	1.328 – 0.095	0.45	0.67	0.89	1.1	1.31	1.52	1.72	1.92	2.12
Mo/Rh/40 – Rh/Rh/25	1.328 – 0.231	0.98	1.46	1.94	2.41	2.87	3.33	3.79	4.24	4.68
Mo/Rh/40 – Rh/Rh/30	1.328 – 0.424	1.56	2.32	3.08	3.83	4.58	5.32	6.05	6.77	7.49
Mo/Rh/40 – Rh/Rh/35	1.328 – 0.666	2.08	3.11	4.13	5.14	6.14	7.13	8.12	9.09	10.06
Rh/Rh/40 – Rh/Rh/20	0.948 – 0.095	0.03	0.05	0.06	0.08	0.09	0.1	0.12	0.13	0.14
Rh/Rh/40 – Rh/Rh/25	0.948 – 0.231	0.03	0.05	0.07	0.08	0.1	0.11	0.13	0.14	0.16
Rh/Rh/40 – Rh/Rh/30	0.948 – 0.424	0.03	0.04	0.05	0.06	0.07	0.09	0.1	0.11	0.12
Rh/Rh/40 – Mo/Mo/20	0.948 – 0.15	0.99	1.47	1.95	2.42	2.88	3.33	3.78	4.22	4.65
Rh/Rh/40 – Mo/Mo/25	0.948 – 0.36	1.8	2.68	3.55	4.42	5.27	6.11	6.95	7.78	8.59
Rh/Rh/40 – Mo/Mo/30	0.948 – 0.641	2.2	3.29	4.36	5.43	6.48	7.53	8.56	9.59	10.6
Rh/Rh/35 – Mo/Mo/25	0.666 – 0.36	1.62	2.41	3.2	3.98	4.75	5.51	6.27	7.01	7.75
Rh/Rh/35 – Mo/Mo/30	0.666 – 0.641	1.89	2.83	3.75	4.67	5.58	6.47	7.36	8.25	9.12
Rh/Rh/40 – Mo/Rh/25	0.948 – 0.309	1.68	2.51	3.33	4.14	4.95	5.74	6.53	7.31	8.08

Table 2: SNR results for microcalcification subtracted images using GdOS scintillator and assuming a 50% adipose and 50% glandular tissue thickness for a 5 cm breast.

Taking into consideration the exposure of High and Low energy images, we are compelled to select the ones that maintain low exposure levels when added together. For example in table 2, Mo/Mo/40 High energy image (where Mo/Mo/40 is anode/filter/voltage) and Rh/Rh/30 Low energy image yields SNR value of 4.6 for 300 μm microcalcification whereas for Rh/Rh/40 HE and Mo/Rh/25 LE yields SNR value of 4.95. The latter value is higher but also its exposure levels when added are

significantly lower; in the first case the exposure is 1.865 R whereas in the second case it's 1.257 R. If we consider that higher exposure values leads to higher mean glandular dose for the patient then it's imperative to keep exposure low.

If we adopt a minimum threshold of 3 in order to be able to detect microcalcifications and maintain a maximum limit of ~1200 mR exposure then, for GdOS scintillator (table 2) we can see that the optimum combination of anode, filter and voltage for High energy is Rh/Rh/35-40 and for low energy is Mo/Mo-Rh/25-30 allowing us to detect microcalcifications the size of 200 μm . If we set the threshold to SNR=5 then the minimum microcalcification size that we can detect is 300 μm .

Combination of HE – LE Anode/Filter/Voltage	Exposure of HE - LE	Microcalcification size in μm									
		100	150	200	250	300	350	400	450	500	
Mo/Mo/40 – Mo/Mo/20	1.441 – 0.15	0.04	0.05	0.07	0.09	0.11	0.12	0.14	0.15	0.17	
Mo/Mo/40 – Mo/Mo/25	1.441 – 0.36	0.04	0.06	0.08	0.1	0.12	0.14	0.16	0.18	0.2	
Mo/Mo/40 – Mo/Mo/30	1.441 – 0.641	0.03	0.04	0.06	0.07	0.08	0.1	0.11	0.12	0.13	
Mo/Mo/40 – Rh/Rh/20	1.441 – 0.095	0.36	0.53	0.71	0.88	1.04	1.21	1.37	1.53	1.68	
Mo/Mo/40 – Rh/Rh/25	1.441 – 0.231	0.75	1.12	1.49	1.85	2.2	2.55	2.9	3.24	3.58	
Mo/Mo/40 – Rh/Rh/30	1.441 – 0.424	1.18	1.75	2.33	2.89	3.45	4.01	4.56	5.1	5.64	
Mo/Mo/40 – Rh/Rh/35	1.441 – 0.666	1.56	2.33	3.1	3.85	4.6	5.35	6.08	6.81	7.53	
Mo/Mo/40 – Rh/Rh/40	1.441 – 0.948	1.89	2.83	3.75	4.67	5.58	6.48	7.37	8.25	9.13	
Mo/Mo/40 – W/La/20	1.441 – 0.687	0.11	0.16	0.22	0.27	0.32	0.37	0.42	0.46	0.51	
Mo/Mo/40 – W/La/25	1.441 – 1.466	0.09	0.13	0.17	0.22	0.26	0.3	0.34	0.38	0.42	
Mo/Rh/40 – Rh/Rh/20	1.328 – 0.095	0.36	0.53	0.71	0.88	1.04	1.21	1.37	1.53	1.68	
Mo/Rh/40 – Rh/Rh/25	1.328 – 0.231	0.75	1.12	1.48	1.84	2.2	2.55	2.9	3.24	3.58	
Mo/Rh/40 – Rh/Rh/30	1.328 – 0.424	1.17	1.75	2.32	2.88	3.44	3.99	4.54	5.08	5.61	
Mo/Rh/40 – Rh/Rh/35	1.328 – 0.666	1.55	2.32	3.07	3.82	4.57	5.3	6.03	6.76	7.47	
Rh/Rh/40 – Rh/Rh/20	0.948 – 0.095	0.02	0.04	0.05	0.06	0.07	0.08	0.09	0.1	0.11	
Rh/Rh/40 – Rh/Rh/25	0.948 – 0.231	0.03	0.04	0.05	0.06	0.07	0.09	0.1	0.11	0.12	
Rh/Rh/40 – Rh/Rh/30	0.948 – 0.424	0.02	0.03	0.04	0.05	0.05	0.06	0.07	0.08	0.09	
Rh/Rh/40 – Mo/Mo/20	0.948 – 0.15	0.79	1.17	1.55	1.92	2.28	2.64	3	3.34	3.69	
Rh/Rh/40 – Mo/Mo/25	0.948 – 0.36	1.37	2.04	2.7	3.36	4.01	4.65	5.29	5.91	6.53	
Rh/Rh/40 – Mo/Mo/30	0.948 – 0.641	1.65	2.46	3.27	4.07	4.86	5.64	6.41	7.18	7.94	
Rh/Rh/35 – Mo/Mo/25	0.666 – 0.36	1.23	1.83	2.43	3.02	3.61	4.18	4.75	5.32	5.88	
Rh/Rh/35 – Mo/Mo/30	0.666 – 0.641	1.42	2.12	2.81	3.5	4.18	4.85	5.52	6.18	6.83	
Rh/Rh/40 – Mo/Rh/25	0.948 – 0.309	1.27	1.9	2.52	3.13	3.74	4.34	4.93	5.52	6.1	

Table 3: SNR results for microcalcification subtracted images using LSO scintillator and assuming a 50% adipose and 50% glandular tissue thickness for a 5 cm breast.

Results from LSO scintillator seem to produce lower values of SNR. More particularly, High energy image Rh/Rh/40 and Mo/Mo/25 yields SNR=3.52 for 200 μm microcalcification size using GdOS whereas the same setting yield SNR=2.7 for LSO scintillator below the SNR=3 threshold.

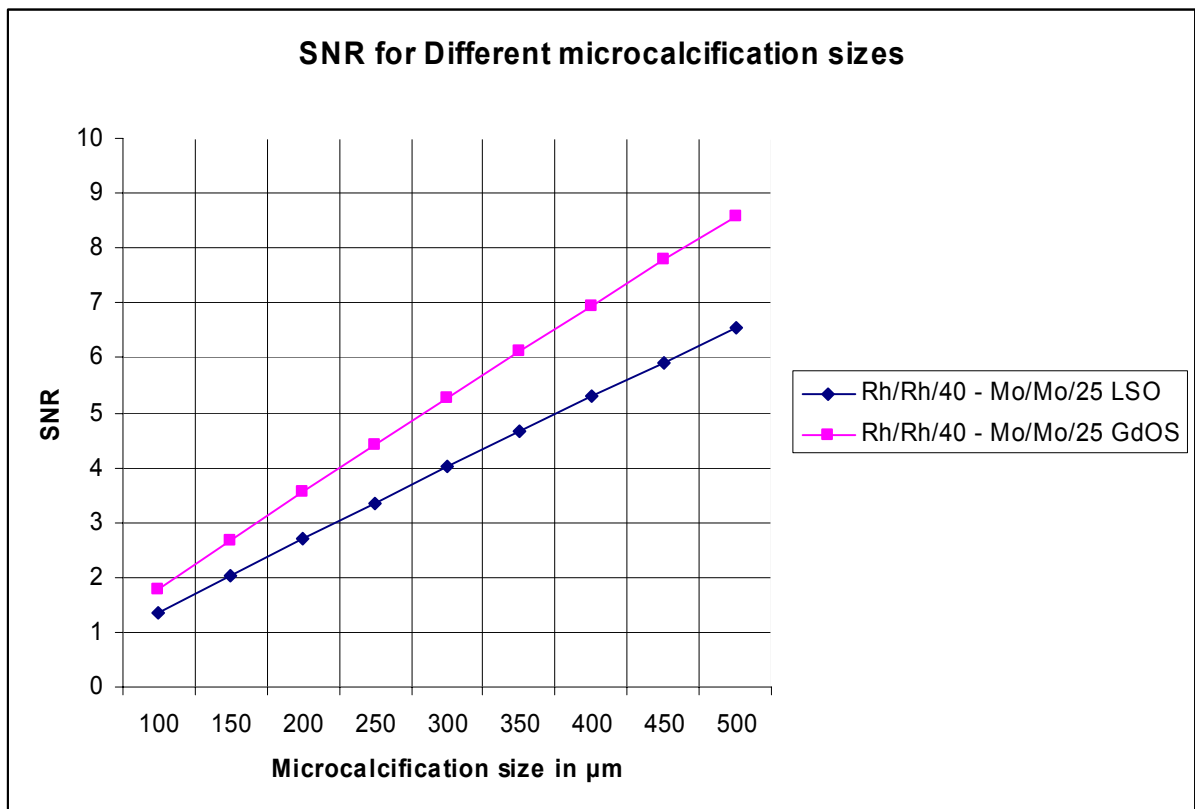
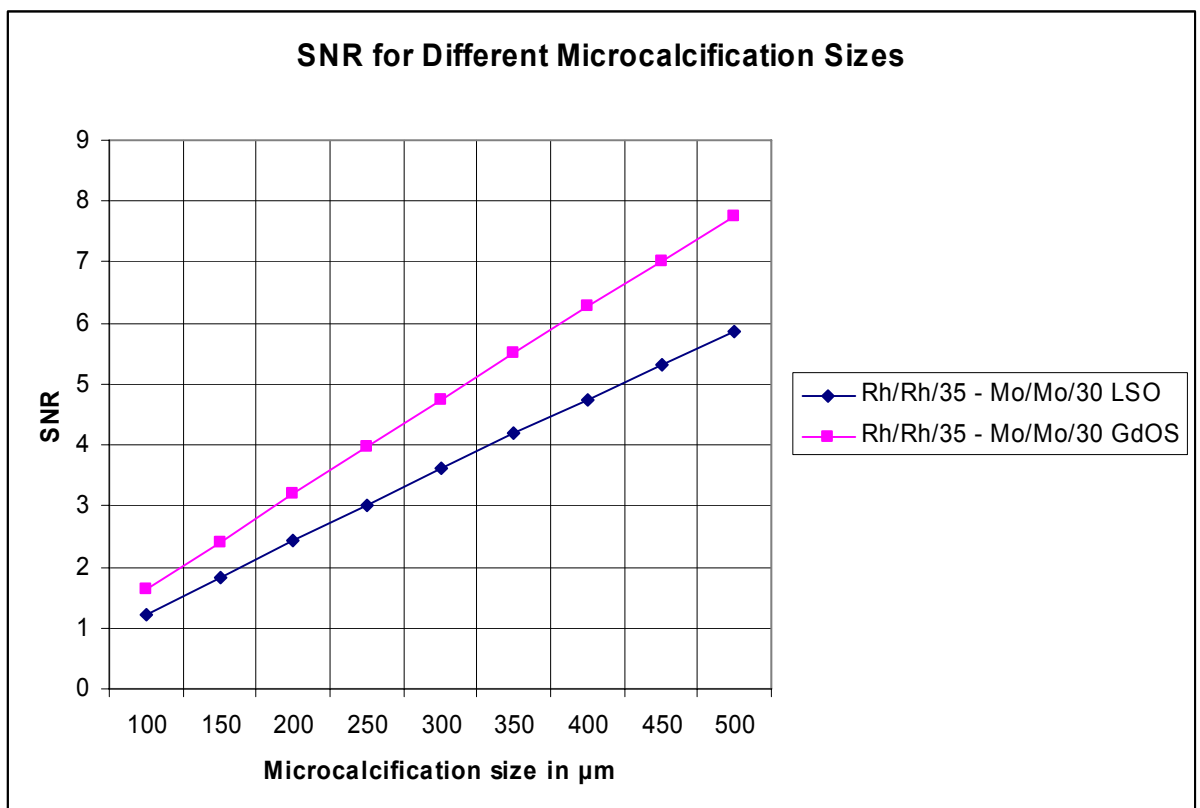


Diagram 1: Chart showing the difference in SNR for LSO and GdOS scintillator



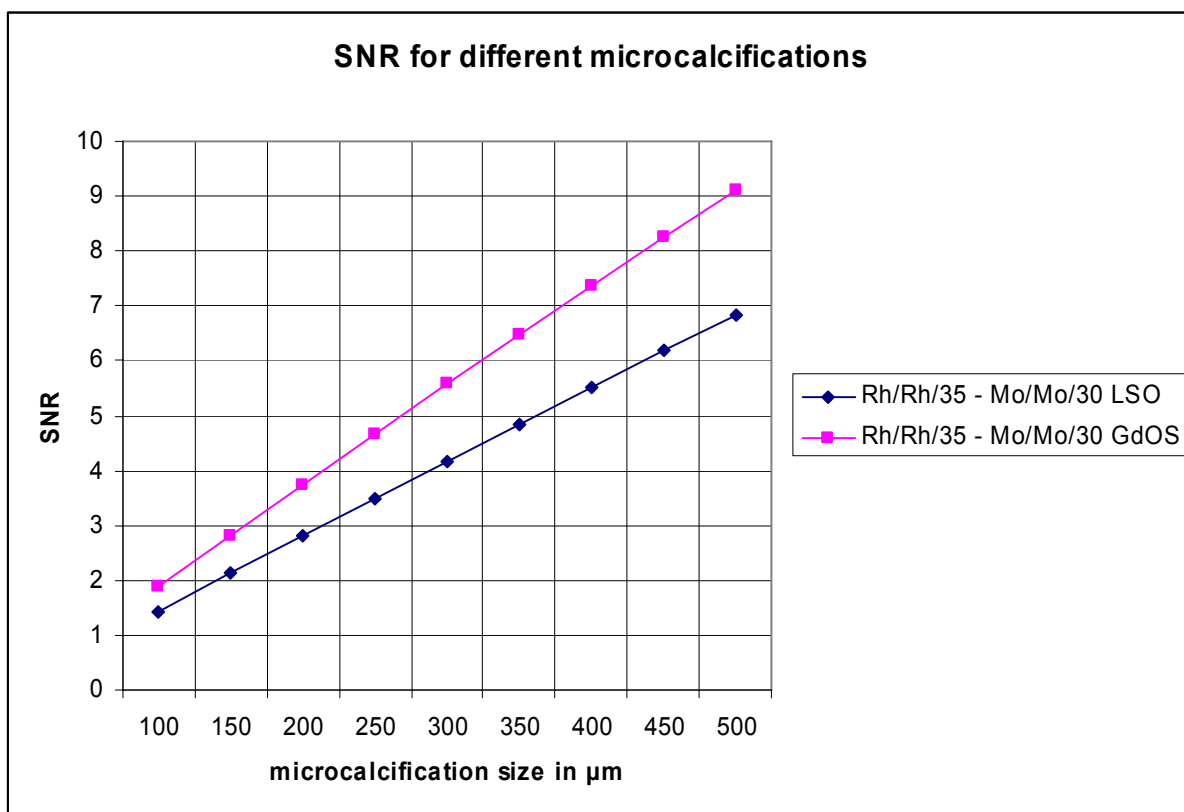


Diagram 3: Chart showing the difference in SNR for LSO and GdOS scintillator

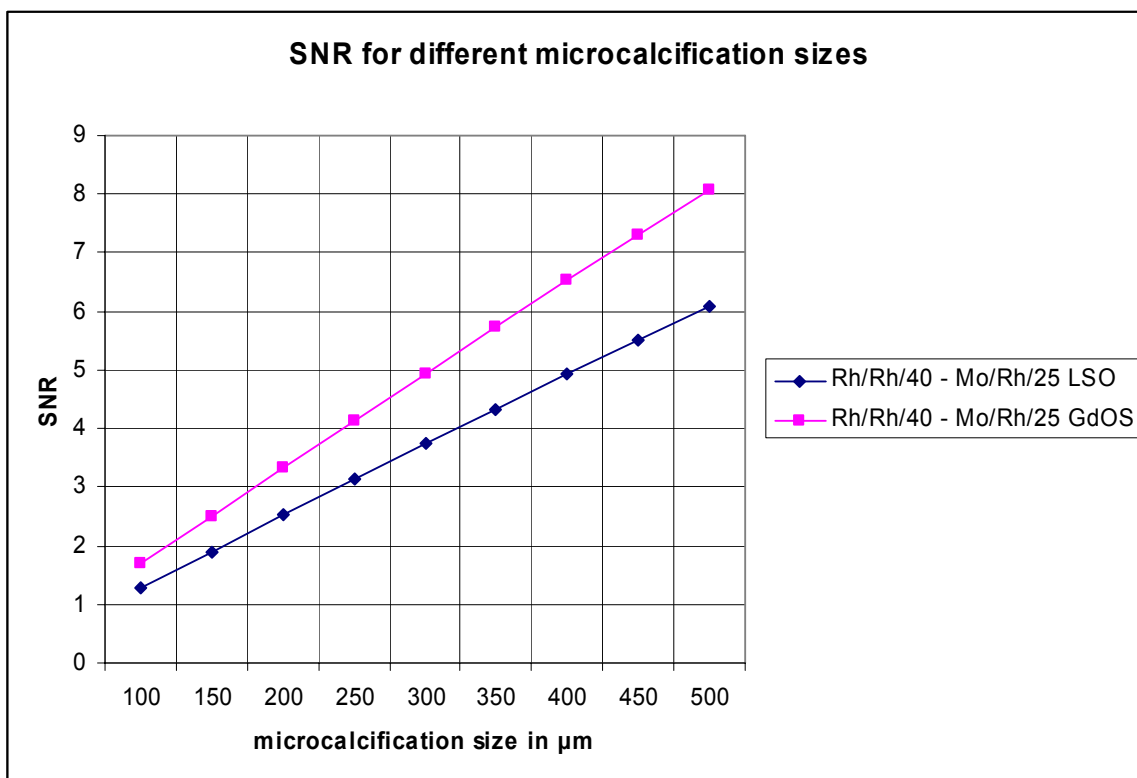


Diagram 4: Chart showing the difference in SNR for LSO and GdOS scintillator

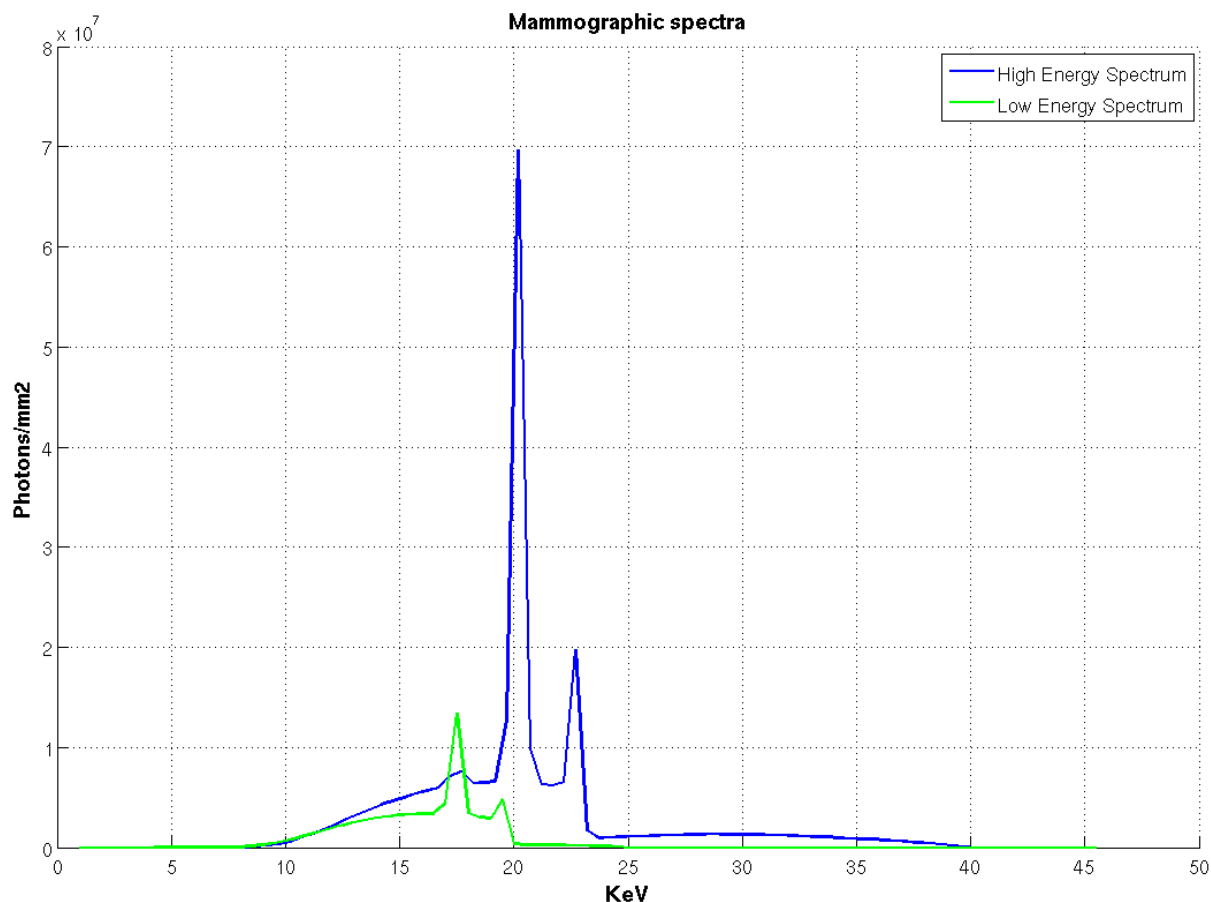


Diagram 5: Rh/Rh/40 spectrum (in blue) and Mo/Mo/25 spectrum (in green). Rhodium filter thickness is 25 μm and Molybdenum filter thickness is 30 μm .

4. Conclusions

This paper described a theoretical framework for calculating the signal to noise ratio in dual energy mammography using tabulated data, simulating attenuation of x rays in breast tissues and modeling the detector performance for two different scintillating materials; GdOS:Tb and LSO:Ce. The present study was a contribution to the optimization of the exposure parameters at Rh/Rh/35-40 for high energy and Mo/Mo-Rh/25-30 for low energy. The performance of the LSO:Ce scintillator based detector showed SNR values than GdOS:Tb.

5. References

- [1] Lemacks R.M., Kappadath S.C., Shaw C.C., Liu X., Whitman G.J., (2002), “A dual-energy subtraction technique for microcalcification imaging in digital mammography”, *Medical Physics*, 29(8), 1739-1751
- [2] Brandan M-E., Ramirez-R V., (2006), “Evaluation of dual energy subtraction of digital mammography images under conditions found in a commercial unit”, *Phys. Med. Biol.* 51, 2307-2320
- [3] Michail C., David S., Liaparinos P., Valais I., Nikolopoulos D., Kalivas N., Toutountzis A., Cavouras D., Kandarakis I., Panayiotakis G, (2007), “Evaluation of the imaging performance of LSO powder scintillator for use in X ray mammography”, *Nucl. Instr. Meth. Phys. Res. A*, 580, 558-561
- [4] David S., Michail C., Valais I., Nikolopoulos D., Liaparinos P., Kalivas N., Kalatzis I., Toutountzis A., Efthimiou N., Loudos G., Sianoudis I., Cavouras D., Dimitropoulos N., Nomikos C.D., Kandarakis I., Panayiotakis G.S., (2007), “Efficiency of LSO powder phosphor as X ray to light converter under mammographic conditions”, *Nucl. Instr. Meth. Phys. Res. A*, 571, 346-349
- [5] Boone M.J., Fewell T.R., Jennings R.J, (1997), “Molybdenum, rhodium and tungsten anode spectral models using interpolating polynomials with application to mammography”, *Medical Physics*, 24(12), 1863-1874
- [6] Storm, E., Israel, H., (1967). “Photon cross-sections from 0.001 to 100 MeV for elements 1 through 100”.
Report LA-3753, Los Alamos Scientific Laboratory, University of California, CA.
- [7] Kandarakis I., Cavouras D., (2001). “Role of the activator in the performance of scintillators used in X ray imaging”. *Applied Radiation and Isotopes* 54, 821-831